Article

J. Biol. Regul. Homeost. Agents. 2024; 38(5): 4427–4438
https://doi.org/10.23812/j.biol.regul.homeost.agents.20243805.352

M1 Macrophage-Derived Exosomes Convert TAMs into an Anti-Tumor M1 Phenotype to Inhibit the Progression of Prostate Cancer

Xuancai Chen[1], Lexi Zhu[1], Shahuang Cao[1], Wei Su[1], Heng Tan[1], Xin Tang[1,*]

[1]Department of Urology, The Affiliated Nanhua Hospital, Hengyang Medical School, University of South China, 421000 Hengyang, Hunan, China
*Correspondence: 18229229383@163.com (Xin Tang)
Published: 1 May 2024

Background: Prostate cancer is the most common and solid malignancy among male tumors worldwide. Converting tumor-associated macrophages (TAMs) into anti-tumor M1 macrophages holds a promising potential for cancer treatment. Therefore, this study investigated whether M1 macrophage-derived exosomes affect prostate cancer progression by inducing TAM reprogramming into M1-like macrophages.

Methods: LPS-induced RAW264.7 cells were polarized into M1-type macrophages. Exosomes isolated from the M1 macrophages (M1-exos) were observed using transmission electron microscopy (TEM), tracked by nanoparticle tracking analysis (NTA), and identified through western blot analysis. After this, M1-exos were co-cultured with human prostate cancer (PC-3) cells and interleukin-4 (IL-4)-induced M2-like macrophages. The effects of M1-exos on prostate cancer progression and TAM polarization were evaluated using cell counting kit-8 (CCK-8), 5-ethynyl-2′-deoxyuridine (EdU), flow cytometry, Transwell, and wound healing assays. Furthermore, to analyze the impact of M1-exos on prostate cancer progression by inducing TAM polarization, *in vivo* xenograft tumor models were constructed, followed by H&E staining, immunohistochemistry, and TdT-mediated dUTP nick end labeling (TUNEL) assays.

Results: We successfully polarized immature M0 macrophages into an M1 phenotype using RAW264.7 cells and obtained M1-exos from these cells. Moreover, findings from both *in vivo* and *in vitro* experiments unveiled that M1-exos inhibited the proliferation ($p < 0.05$), invasion ($p < 0.05$), and migration of prostate cancer cells ($p < 0.05$). Additionally, M1-exos promoted apoptosis ($p < 0.05$) and induced the polarization of TAM into M1-type macrophages.

Conclusion: M1-exos induced the polarization of TAM into the M1 phenotype with anti-tumor potential, thereby suppressing prostate cancer growth and metastasis. Therefore, M1-exos hold promising potential for treating prostate cancer.

Keywords: prostate cancer; exosomes; macrophage polarization; tumor growth and metastasis

Introduction

Prostate cancer (PC) is a common and solid malignancy among men worldwide, posing a serious threat to human health and life. PC ranks second among male malignant tumors in terms of incidence [1]. Over the past decades, its incidence and mortality rates have been gradually increased [2]. Current data demonstrate that approximately 1.1 million new cases of PC are diagnosed annually worldwide, with a significant case fatality rate of about 12.46%, severely affecting the physical and mental health of men [3]. Although existing treatment approaches for localized PC, including radical prostatectomy, chemotherapy, radiotherapy, immunotherapy, and androgen deprivation therapy (ADT), can extend patient survival, they remain unsatisfactory [4]. Therefore, gaining a comprehensive understanding of the specific pathogenesis of PC is really important to explore novel treatment methods in its clinical management.

Tumor cells reside in both the internal and external tumor environment, affecting tumor occurrence and metastasis. The composition of the tumor tissue environment includes crucial components such as the structure, function, and metabolism of tumor tissues. Furthermore, this environment encompasses tumor cells, tumor-associated macrophages (TAMs), tumor-associated fibroblasts, mast cells, immune cells, and active mediators [5,6]. Specifically, TAMs are a group of inflammatory cells extensively infiltrating within the tumor microenvironment (TME) [7]. Under the influence of the microenvironment, both *in vivo* and *in vitro*, macrophages usually undergo polarization into two phenotypes, the anti-tumor M1 and the oncogenic M2 macrophages, both contributing to tumor initiation and progression. Research has indicated that M2 macrophages play a pivotal role in promoting tumor metastasis. Furthermore, the cytokine interleukin-10 (IL-10), secreted by M2 macrophages, exerts anti-inflammatory and tissue-repairing effects, restraining the immune response

Journal of
BIOLOGICAL REGULATORS
and Homeostatic Agents

within the TME and impairing the functions of NK cells and cytotoxic T lymphocytes, thereby assisting tumor cells in evading the immune system [8].

Additionally, M1 macrophages exert anti-tumor effects by secreting pro-inflammatory cytokines that antagonize the action of M2 macrophages within the TME [9]. Specifically, M1 macrophage polarization has been reported to exert anti-tumor effects in PC [10,11]. However, the precise mechanism regulating macrophage polarization in PC is yet to be elucidated.

Exosomes are a subtype of membrane-bound vesicles with diameters between 40 and 200 nm. They have been extensively studied due to their involvement in intracellular communication, particularly in tumor development [12]. Exosomes comprise various biologically active molecules, including miRNAs, non-coding RNAs, proteins, and lipids. These exosomal contents can be absorbed by recipient cells through autocrine and paracrine signaling pathways, leading to functional changes in target cells and playing essential roles in diverse cellular processes [13,14]. Currently, research on the regulation of macrophage polarization by exosomes primarily focuses on exosomes derived from mesenchymal stem cell, tumor cell, or their contents that regulate macrophage polarization in cancer progression. However, there is a scarcity of research investigating the role of exosomes derived from macrophages themselves in regulating their polarization. Interestingly, recent findings have found that M1 macrophage-secreted exosomes can reprogram M2 macrophages to M1, thereby inhibiting tumor progression [15]. Therefore, we proposed that M1 exosomes might serve as a new therapeutic approach for treating PC by regulating macrophage polarization.

This study aimed to investigate the impact of M1 macrophage-secreted exosomes on the reprogramming of TAMs into the M1 phenotype and to explore the effects of this reprogramming on the growth, invasion, and metastasis of PC by constructing both *in vitro* and *in vivo* models.

Methodology and Materials

Cell Culture and Treatment

We obtained a murine macrophage cell line (RAW264.7) from Sunncell (Wuhan, China) and a PC cell line (PC-3) from Procell Life Science & Technology Co., Ltd. (Wuhan, China). These cells were cultured in dulbecco's modification of eagle's medium (DMEM, D0822, Sigma-Aldrich, St. Louis, MO, USA) medium containing 10% fetal bovine serum (TMS126, Sigma-Aldrich, St. Louis, MO, USA), and incubated at 37 °C in a humidified atmosphere with 5% CO_2.

RAW264.7 Polarization Induction

Polarization of RAW264.7 cells (immature M0 macrophages) into the M1 phenotype was induced following a previously described method [16]. For this purpose, RAW264.7 cells were cultured until reaching approximately 80% confluence. Subsequently, the cells underwent a 24-hour exposure to 100 ng/mL LPS (Sigma-Aldrich, St. Louis, MO, USA) and 20 ng/mL interferon (IFN)-γ (Sigma-Aldrich, St. Louis, MO, USA). Furthermore, for induction of M2-polarized macrophage, RAW264.7 cells were treated with 20 ng/mL IL-4 (Sigma-Aldrich, St. Louis, MO, USA).

PC-3 Treatment

PC-3 cells in the logarithmic growth phase were digested with 0.1% trypsin, followed by staining with trypan blue for cell counting. A cell suspension was prepared at a density of 1.0×10^7 cells/mL for injection into nude mice. The cells underwent STR profiling and were tested negative for contamination using mycoplasma testing. All manipulations were conducted using aseptic techniques to maintain cell purity and prevent contamination.

Extracellular Vesicle Extraction and Isolation

After the successful induction of M1 macrophages, the culture medium was replaced with DMEM without exosome-free serum, and cells were cultured in a flask for 48 hours. The cells and culture medium were then collected, and extracellular vesicles were isolated and separated using an Exo extraction kit (Thermo Fisher Scientific, Waltham, MA, USA) following the manufacturer's instructions. The extracellular vesicles were deposited onto a copper grid, the supernatant was removed after precipitation, and uranyl acetate was added. After air-drying at room temperature, the morphology of the extracellular vesicles was examined utilizing TEM (JEM-1400Flash, Japan Electronics Corporation, Tokyo, Japan). Finally, a nanoparticle tracking analyzer (ZetaView, Particle Metrix, Shanghai, China) was employed to analyze the concentration and size of the extracellular vesicles.

Establishment of in Vivo Prostate Cancer Tumor Model

BALB/C mice (n = 16), aged 6–8 weeks and weighing 25 g, were purchased from Hunan Srek Jingdong Co., Ltd. They were acclimatized for one week and subsequently received a subcutaneous injection. PC-3 cells in the logarithmic growth phase from each group were prepared as a cell suspension at a density of 1×10^7 cells/mL in DMEM medium. Each mouse was injected subcutaneously with 0.2 mL of the cell suspension in the left forelimb. Tumor formation was observed on the 7th day after modeling. The mice were randomly divided into two groups: the Model group and the M1-exos group. Starting one week after tumor inoculation, the M1-exos group of mice was intravenously administered extracellular vesicles (100 μg in 150 μL phosphate buffered saline (PBS, P2272, Sigma-Aldrich, St. Louis, MO, USA) every 3 days, and the control group mice received an equivalent volume

of PBS. A vernier caliper was used to measure the length and width of each tumor on days 3, 5, 7, 9, 11, 13, 15, 17, 19, and 21 after tumor inoculation. The tumor volume was calculated using the following formula: tumor volume = (length [mm])^2 × (height [mm]) × π/6. A tumor growth curve was plotted. After 2 weeks of oral administration, mice were euthanized with 3% pentobarbital sodium (200 mg/kg, 1012365C, Thermo Fisher Scientific, Waltham, MA, USA) to ensure complete removal of the tumor in a cold environment. Subsequently, surface fat tissue was excised, and tumors were weighed. The tumors were then sectioned into appropriate sizes, fixed with paraformaldehyde (10015264C, Thermo Fisher Scientific, Waltham, MA, USA), and subjected to hematoxylin and eosin (H&E) staining and immunohistochemistry analysis.

H&E Staining

Tumor tissues isolated from different groups of mice were individually fixed in paraformaldehyde for 24 hours and embedded in paraffin. Tissue sections were deparaffinized with xylene for 10 minutes, followed by dehydration using decreasing ethanol concentrations and rinsing with distilled water. After this, tissues were stained with hematoxylin for 7 minutes and eosin for 2 minutes. After dehydration with increasing ethanol concentrations, the tissue was mounted with resin. Finally, the stained tissue sections were observed using an optical microscope (V1.8.0.112, NIH, Madison, WI, USA).

Immunohistochemistry (IHC)

Tissue specimens obtained from different tumor groups were fixed in paraformaldehyde for 24 hours and subsequently embedded in paraffin and sectioned. They were deparaffinized using xylene and ethanol, followed by rinsing with PBS. The sections were then blocked for 30 minutes in goat serum working solution and incubated overnight with the primary antibody against Ki67 (1:1000, A20018, Abclonal, Wuhan, China) at 4 °C. After this, the sections were incubated with secondary antibodies at 37 °C for 40 minutes. The tissue sections were counterstained with 3,3-diaminobenzidine (DAB) and hematoxylin. Finally, the sections were dehydrated, cleared, and mounted for observation.

Enzyme-Linked Immunosorbent Assay (ELISA)

The levels of tumor necrosis factor-α (TNF-α, RM17776, Abclonal, Wuhan, China), IL-6 (RK00004, Abclonal, Wuhan, China), and IL-1β (RK00001, Abclonal, Wuhan, China) in the cell supernatant were assessed following the instructions provided with respective kits. The optical density (OD) of each well was determined at 450 nm by an ELISA plate reader. Moreover, the cellular levels of tumor necrosis factor-α (TNF-α), IL-6, and IL-1β were determined based on a standard curve.

Cell Proliferation Assay

Cellular viability was assessed using cell counting kit-8 (CCK-8) assay. After the indicated treatment, PC-3 cells were seeded into 96-well plates at a density of 2 × 10^3 cells/100 µL. Following incubation, 20 µL of CCK-8 reagent was added to each well at 12, 24, and 48 hours and underwent an additional one-hour incubation in the dark. The viability of each group of PC-3 cells was examined by assessing the absorbance at 450 nm using a microplate reader.

5-ethynyl-2′-deoxyuridine (EdU) Assay

PC-3 cells were seeded onto 96-well plates, subsequently fixed, and permeabilized. After this, the cells were treated with EdU (50 µM) (Sigma-Aldrich, St. Louis, MO, USA) and then incubated with 4′,6-diamidino-2-phenylindole (DAPI, 3 µg/mL) (Sigma-Aldrich, St. Louis, MO, USA). Finally, the cells were observed using a fluorescence microscope (DM3000, Leica, Wetzlar, Germany).

Immunofluorescence Staining

After the indicated treatment, PC-3 cells were collected and washed three times with PBS, subsequently fixed with 4% paraformaldehyde at room temperature for 15 minutes. After this, cells were incubated with 1% Triton X-100 for 10 minutes, followed by blocking in 1% bovine serum albumin. The cells were then incubated overnight with primary antibodies against improved neds operating system (iNOS, 1:200, ab178945, Abcam, Cambridge, UK), Agr1 (1:100, ab96183, Abcam, Cambridge, UK), PKH-67 (1:100, ab276727, Abcam, Cambridge, UK) at 4 °C. After washing three times with PBS, the cells underwent incubation with Alexa Fluor 488-goat anti-mouse IgG secondary antibody (1:500, Life Technologies, New York, NY, USA). Following Phalloidin (1:1000, ab176753, Abcam, Cambridge, UK) staining, cells were washed with PBS, and nuclei were stained with DAPI. Finally, the cells were observed utilizing a Nikon A1R confocal microscope (DM6B, Leica, Wetzlar, Germany).

Transwell Assay

PC-3 cells from each experimental group were seeded into the upper chamber of Matrigel-coated Transwell inserts. Meanwhile, the lower chamber was filled with 600 µL of DMEM containing 10% FBS. After 24 hours of incubation at 37 °C, cells were washed with PBS. Those cells remaining on the upper side were fixed with 4% paraformaldehyde, stained with 0.1% crystal violet dye (10511230, Thermo Fisher Scientific, Waltham, MA, USA), and washed with tap water for 30 seconds to 1 minute. Furthermore, after mounting with neutral resin, the membranes were observed employing an inverted microscope (Olympus, Tokyo, Japan). Image J software (V1.8.0.112, NIH, Madison, WI, USA) was used to assess the number of invasive cells.

Journal of
BIOLOGICAL REGULATORS
and Homeostatic Agents

Scratch Assay

PC-3 cells from each experimental group were seeded at a density of 5×10^5 cells/well into 6-well plates and incubated overnight at 37 °C. The wells were marked with a marker pen to create evenly spaced lines crossing the entire well, maintaining intervals of approximately 0.5–1 cm, with at least 5 lines per well. Upon achieving a cell confluence of 80%, a 200 µL pipette tip was used to create a straight scratch on the bottom. After washing three times with PBS, each well was added with a serum-free medium. The scratches were observed utilizing a microscope (Olympus, Tokyo, Japan) at 0 and 24 hours, and quantified using Image J software (V1.8.0.112, NIH, Madison, WI, USA).

Flow Cytometry Apoptosis Analysis

The cells from each group were centrifuged at 1000 rpm for 5 minutes. Subsequently, the cells were resuspended in 100 µL of binding buffer, followed by adding 5 µL of Annexin V-FITC and an equal amount of propidium iodide (PI). For assessing macrophage polarization, the cells were incubated with fluorescently labeled antibodies against specific polarization markers, including recombinant tetraspanin 30 cluster of differentiation 86 (CD86, ab239075, Abcam, Cambridge, UK), F4/80 (ab237335, Abcam, Cambridge, UK), CD163 (ab182422, Abcam, Cambridge, UK), CD14 (ab28061, Abcam, Cambridge, UK) for M1 macrophages and PKH-67 (ab276727, Abcam, Cambridge, UK). After incubation, apoptotic cells were detected using a flow cytometer. The parameters were set as follows: temperature 4 °C, speed 1000 rpm, centrifugation 5 minutes.

TdT-Mediated dUTP Nick End Labeling (TUNEL) Assay

Following treatment with the TUNEL detection solution, the slides were rinsed with PBS and then incubated with 4′,6-diamidino-2-phenylindole (DAPI) staining solution for 5 minutes at room temperature in the dark. DAPI is a fluorescent dye commonly used for DNA labeling, facilitating the visualization of nuclei. After DAPI staining, the slides were rinsed with PBS and mounted on glass coverslips. The fluorescence signals of both TUNEL and DAPI were observed and captured using a fluorescence microscope (DM3000, Leica, Wetzlar, Germany).

Western Blotting

After total protein extraction, proteins were quantified using a BCA kit. The protein samples were resolved through SDS-PAGE and were subsequently transferred onto a PVDF membrane. The membrane was blocked with TBET containing 5% skim milk, followed by four washes with TBST, and then incubated with antibodies against CD63 (1:500, ab2862515, Abclonal, Wuhan, China), tumor susceptibility gene 101 (TSG101, 1:500, ab2863517, Abclonal, Wuhan, China), and Alix (1:1000, ab2862515, Abclonal, Wuhan, China) at 4 °C. The next day, the membrane was incubated with secondary antibodies at room temperature for 1 hour. After washing, protein bands were visualized utilizing an ECL reagent. Finally, these bands were analyzed and quantified using Image J software (V1.8.0.112, NIH, Madison, WI, USA).

Statistical Analysis

Data analyses were conducted using GraphPad Prism 9 (Dotmatics, Boston, MA, USA) software. Normally distributed data were presented in quantitative graphs as mean ± SD. Differences between the two groups were determined through an independent sample *t*-test. Moreover, multiple group comparisons were performed using a one-way analysis of variance (ANOVA). Furthermore, SPSS 22 (IBM, Corp., Armonk, NY, USA) was employed for multiple post-hoc comparisons. Statistical significance was defined at a p-value < 0.05.

Result

Identification of M1 Exos and their Uptake by PC-3 Cells

For the induction of macrophage polarization to M1, immature macrophages (M0 RAW 264.7) were treated with LPS for 24 hours to induce M1 RAW 264.7 (Fig. 1A). Compared to M0 cell models, M1 cell models showed a significant accumulation of TNF-α, IL-1β, and IL-6 ($p < 0.05$; Fig. 1B), indicating successful polarization of M0 into M1 phenotype. Subsequently, M1 exosomes were obtained through centrifugation. Transmission electron microscopy results showed that M1 exosomes exhibited a classical cup-shaped vesicle morphology (Fig. 1C). Based on nanoparticle tracking analysis (NTA) data, the peak particle size of M1-Exos ranged from 90 to 220 nm, with a maximum count of 1.38×10^5 particles/mL. The volume distribution of M1-Exos was predominantly concentrated between 100 and 400 nm, indicating a concentrated and uniform size distribution of the extracted M1-Exos (Fig. 1D). Protein imprinting demonstrated significantly elevated expression levels of exosomal marker proteins TSG101 ($p < 0.05$) and Alix ($p < 0.05$; Fig. 1E) in M1-Exos. However, there was no statistical difference in CD63 levels ($p > 0.05$). Furthermore, co-culturing M1-Exos with PC-3 cells revealed that PC-3 cells could uptake M1-Exos (Fig. 1F,G). These findings suggest the successful isolation of M1-Exos and the efficient internalization of M1-Exos by PC-3 cells.

M1-Exos Inhibit Prostate Cancer Cell Growth and Metastasis

Next, we examined the role of M1-Exos in PC-3 cell growth and metastasis. The CCK-8 assay revealed that M1-Exos significantly inhibited PC-3 proliferation ($p < 0.05$; Fig. 2A). Similarly, EdU assay results showed a significant reduction in the proliferation of PC-3 cells in the M1-Exos

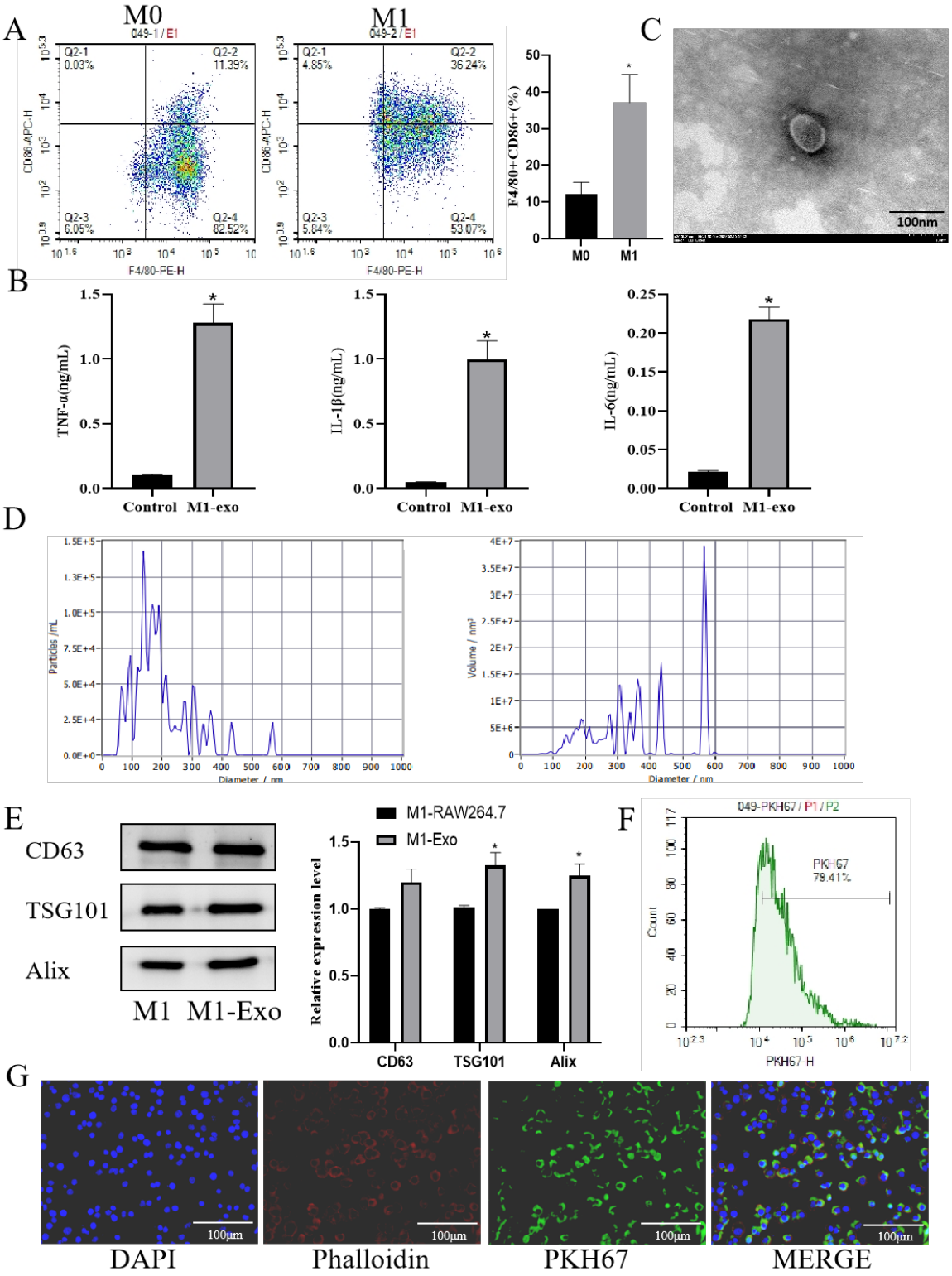

Fig. 1. Isolation and identification of M1 exos and their uptake by PC-3 cells. (A) Flow cytometry distinguished M0 RAW 264.7 and M1 RAW 264.7 cells. (B) ELISA detected expression of TNF-α, IL-1β, and IL-6 in cell supernatant. (C) Transmission electron microscopy observed exosomes. (D) NTA analysis of exosome diameter and concentration. (E) Western blot analysis detected the expression of exosome marker proteins CD63, TSG101, and Alix. (F) The expression of PKH-67 was determined using flow cytometry. (G) Immunofluorescence traced the uptake of M1-Exos by PC-3 cells. * $p < 0.05$. PC, prostate cancer; TNF-α, tumor necrosis factor-α; IL, interleukin; NTA, nanoparticle tracking analysis; DAPI, 4′,6-diamidino-2-phenylindole; ELISA, enzyme-linked immunosorbent assay.

Journal of
BIOLOGICAL REGULATORS
and Homeostatic Agents

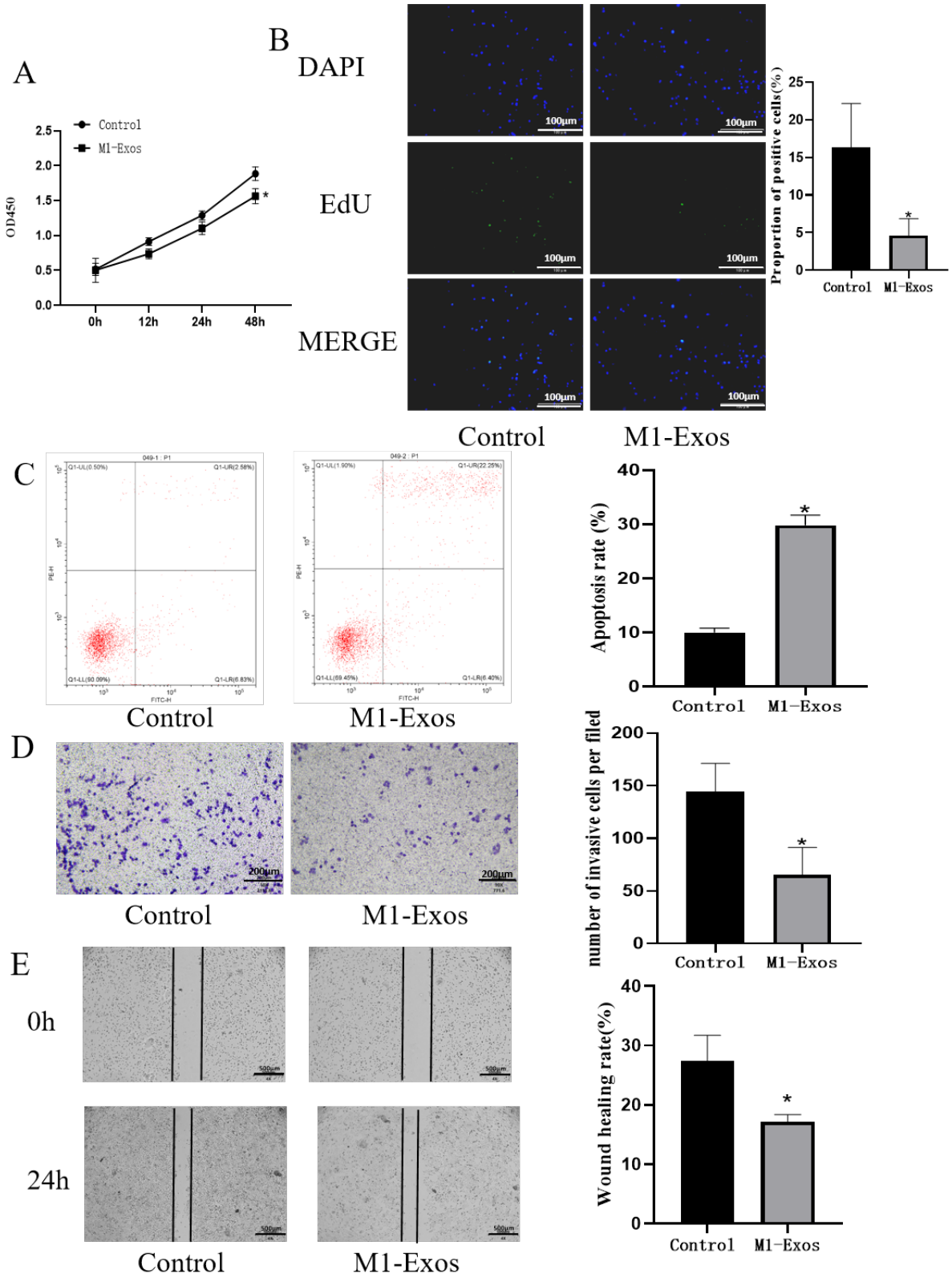

Fig. 2. M1-Exo inhibits prostate cancer cell growth and metastasis. (A) CCK-8 assay detected the proliferation of PC-3 cells. (B) EdU detected the proliferation of PC-3 cells. (C) Flow cytometry was used to evaluate apoptosis of PC-3 cells. (D) Transwell assay was utilized to assess the invasion capability of PC-3 cells. (E) The wound healing experiment was used to evaluate the migration capability of PC-3 cells. n = 3. * $p < 0.05$. CCK-8, cell counting kit-8; EdU, 5-ethynyl-2′-deoxyuridine.

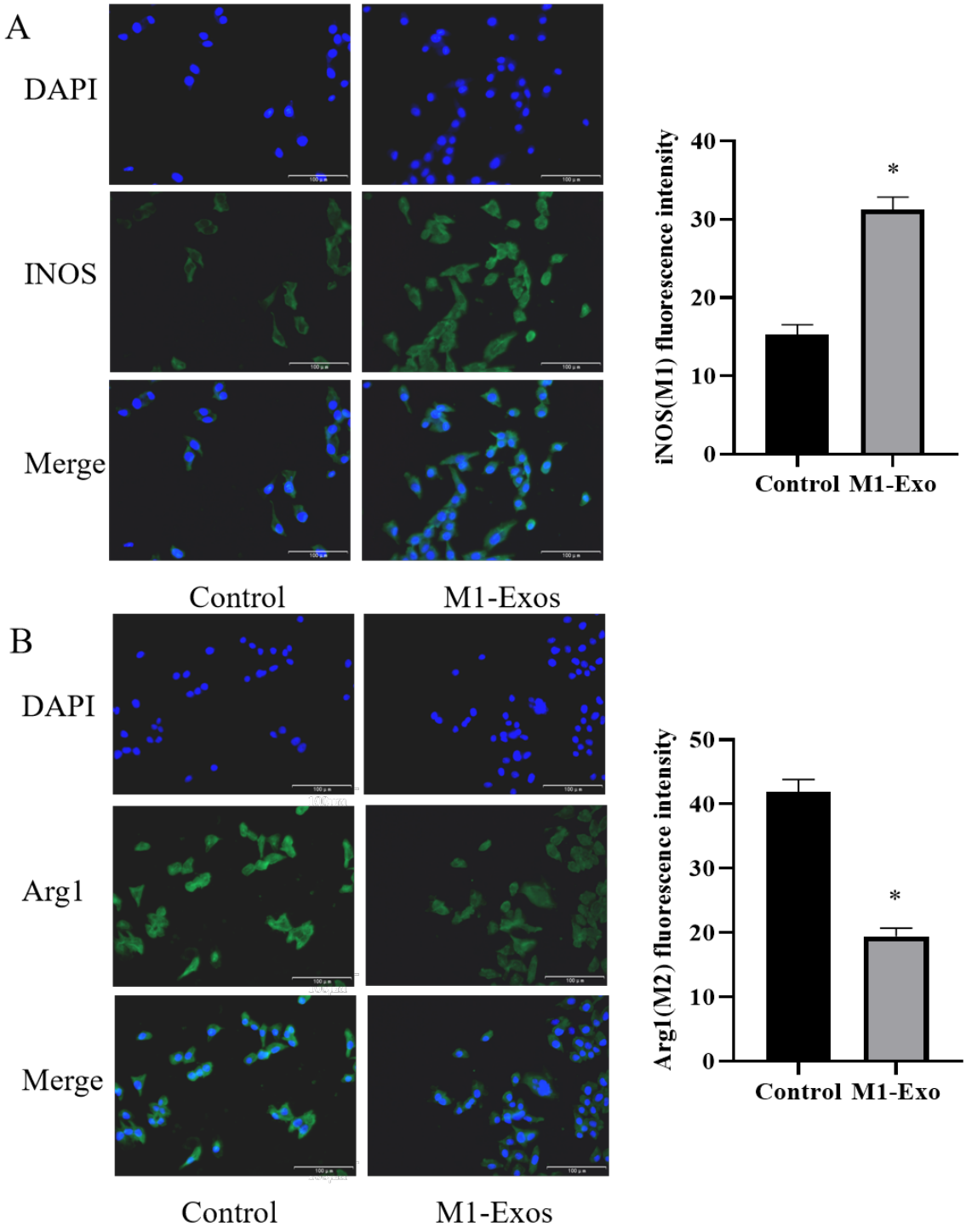

Fig. 3. M1-Exo promotes polarization of TAMs into M1-like macrophages. (A) Immunofluorescence detected expression of iNOS in PC-3 cells. (B) Immunofluorescence detected expression of Arg1 in PC-3 cells. n = 3. * $p < 0.05$. TAMs, tumor-associated macrophages; iNOS, inducible nitric oxide synthase; Arg1, arginase-1.

group ($p < 0.05$; Fig. 2B). Moreover, M1-Exos significantly promoted apoptosis in PC-3 cells ($p < 0.05$; Fig. 2C). Additionally, the Transwell assay indicated that compared to the control group, the M1-Exos group exhibited a significant reduction in the number of invasive PC-3 cells ($p < 0.05$; Fig. 2D). Furthermore, M1-Exos treatment decreased the healing rate of cell wounds 24 hours after scratching ($p < 0.05$; Fig. 2E). These findings demonstrate the inhibitory effect of M1-Exos on the growth and metastasis of PC-3 cells.

Journal of
BIOLOGICAL REGULATORS
and Homeostatic Agents

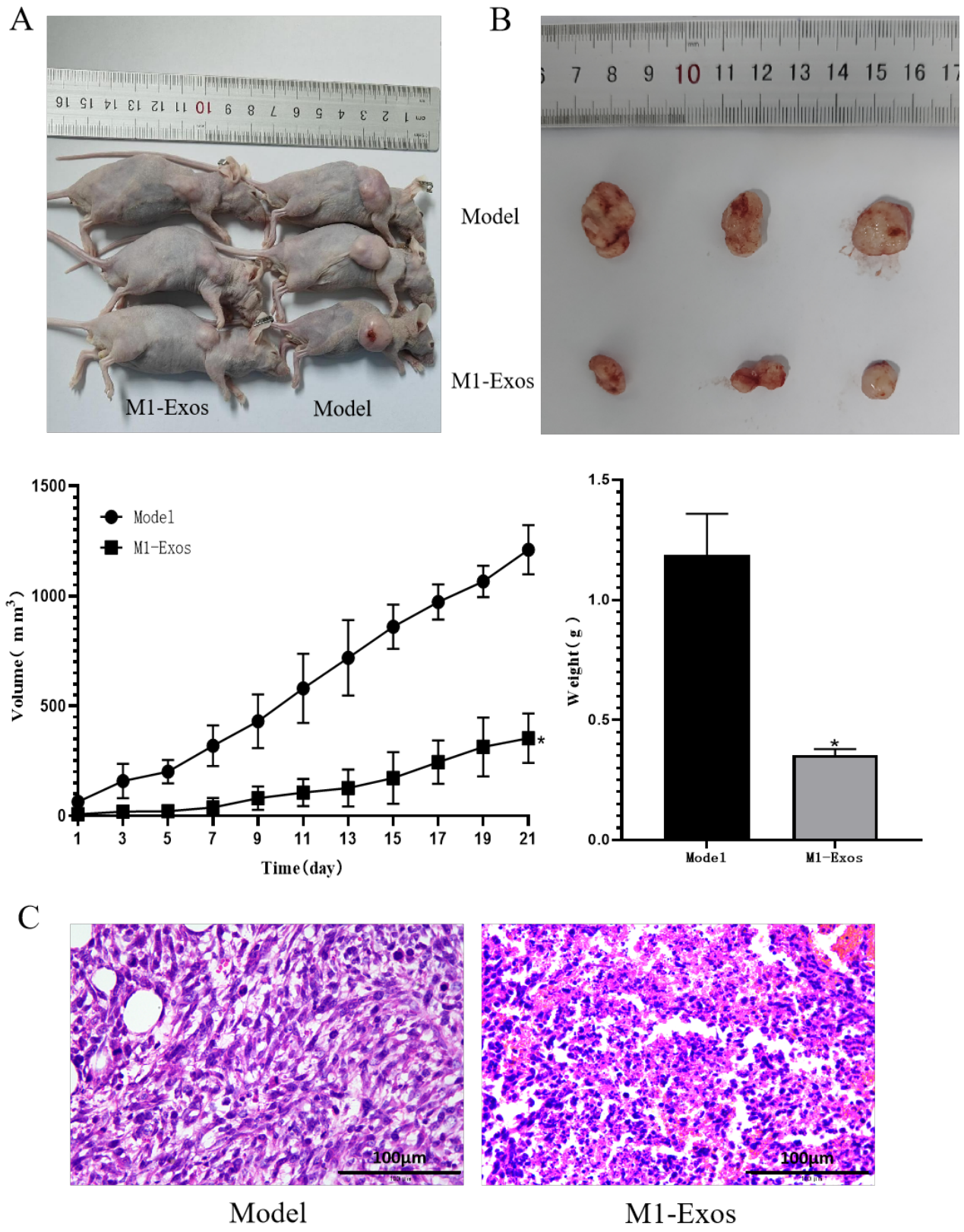

Fig. 4. M1-Exos inhibit prostate cancer cell growth *in vivo*. (A,B) Establishment of BALB/C mice carrying PC-3 cells to evaluate the effect of M1 exos on tumor volume and weight of PC-3 cells. (C) H&E staining was used to evaluate glandular tissue pathology. n = 3. * $p < 0.05$. H&E, hematoxylin and eosin.

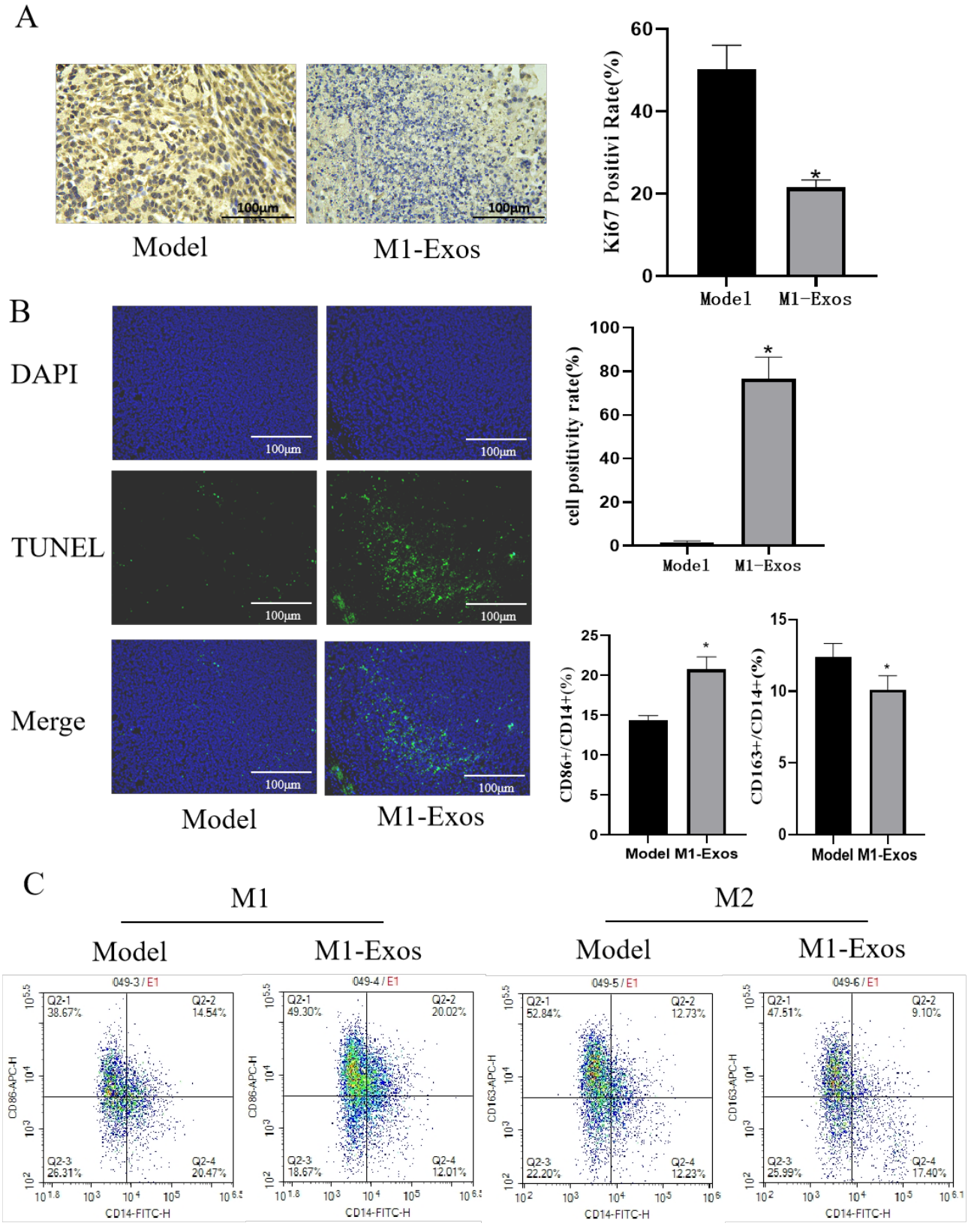

Fig. 5. M1-Exo promotes polarization of TAMs into M1-like macrophages, inhibiting the proliferation of prostate cancer cells and promoting cell apoptosis. (A) IHC detected expression levels of Ki67 in tumor tissue. (B) TUNEL detected apoptosis of cancer cells in tumor tissue. (C) Flow cytometry evaluated polarization of M1 and M1-like macrophages. n = 3. * $p < 0.05$. IHC, immunohistochemistry; TUNEL, TdT-mediated dUTP nick end labeling.

Journal of
BIOLOGICAL REGULATORS
and Homeostatic Agents

M1-Exo Promotes the Reprogramming of TAMs into M1-Phenotype

It is widely recognized that M2-like TAMs can be stimulated, thereby accelerating tumor growth by producing an immunosuppressive TME [17]. To assess the role of M1-Exos on polarization of TAMs, M2 polarized macrophages were induced by treating RAW 264.7 cells with IL-4 to analyze changes in the expression of M1 and M2 markers. As expected, compared to the control group, macrophages treated with M1-Exos exhibited increased levels of the M1 macrophage marker iNOS ($p < 0.05$; Fig. 3A). On the contrary, macrophages treated with M1-Exos showed downregulation in the expression of the M2 macrophage marker Arg-1 (Fig. 3B). These findings are consistent with previous research, demonstrating that M1-Exos contain active components derived from M1 macrophages, enabling them to induce phenotypic switching in macrophages towards the M1 phenotype, developing a local immunostimulatory microenvironment [18]. These experimental results show that M1-Exos promote TAMs towards M1-like macrophages, which could benefit cancer therapy by reversing immune suppression within the TME.

M1-Exos Inhibit Prostate Cancer Cell Growth in Vivo

To validate the tumor-suppressive efficacy of M1-Exos *in vivo*, animal models were established by injecting BALB/C mice bearing PC-3 cells with either PBS or M1-Exos. The tumor volume ($p < 0.05$) and weight ($p < 0.05$) were significantly reduced in the M1-Exos-treated mice compared to those in the control group (Fig. 4A,B), indicating a substantial inhibitory effect of M1-Exos on tumor growth. Furthermore, H&E staining results showed that glandular tissue in the Model group exhibited irregular contours, structural disorders, and significantly increased cell nucleus size, whereas these abnormalities were significantly reversed after M1-Exos treatment (Fig. 4C). These results demonstrate the inhibitory effects of M1-Exos on prostate cancer growth *in vivo*.

M1-Exos Promote TAMs to Polarize towards M1-Like Macrophages, Inhibit Prostate Cancer Cell Proliferation and Promote Cell Apoptosis

We further investigated the effect of M1-Exos on the growth of PC-3 cells *in vivo*. Immunohistochemical analysis showed substantially alleviated expression level of the proliferation marker Ki67 following M1-Exos treatment ($p < 0.05$; Fig. 5A). Additionally, TUNEL staining revealed a significant increase in PC-3 cell apoptosis after M1-Exos treatment ($p < 0.05$; Fig. 5B). Importantly, we observed an increase in M1-like macrophages and a decrease in M2-like macrophages following M1-Exos treatment (Fig. 5C). These findings indicate that M1-Exos promote TAM polarization towards M1-like macrophages, thereby leading to the inhibition of PC cells growth.

Discussion

PC has become the second most destructive tumor affecting male health following lung cancer [19]. TAMs are the essential components within the TME and are associated with the progression of PC [20]. However, the underlying mechanisms and targeted treatment strategies for TAMs in PC remain unclear. This study reports that exosomes secreted by M1 macrophages induce TAM reprogramming into M1-like macrophages, significantly inhibiting the growth, invasion, and metastasis of PC. These observations provide new insights into the clinical management of PC.

Macrophages, essential components of the immune system, are a functionally heterogeneous and highly plastic cell population, representing the most abundant inflammatory cells infiltrating the TME [21]. Increasing evidence suggests the crucial role of M1/M2 polarization in macrophages in driving the malignant progression of PC. For example, enhancer of zeste homolog 2 (EZH2) has been indicated to reverse the resistance of PC to PD-1 CPI by increasing the intratumoral transport of activated CD8 T cells, concomitantly increasing M1 tumor-associated macrophages [22]. Additionally, platinum group elements have been shown to inhibit M1 polarization stimulated by LPS and interferon-γ while promoting M2a polarization mediated by interleukin-4, thereby exerting anti-inflammatory and anti-tumor effects [6]. In most cases, the reprogramming of macrophages from M2 to M1 within the TME is an important strategy for cancer treatment [23]. This study successfully isolated exosomes from M1 macrophages and investigated whether M1 macrophages can influence the TAM reprogramming in the progression of PC through the secretion of these exosomes.

Exosomes, small vesicles secreted by cancer cells and different other cell types, enter surrounding biofluids [24]. They play a crucial role in mediating intercellular communication within the TME, particularly involving TAMs during cancer progression. For example, MSC-derived exosomes have been indicated to enhance drug resistance in breast cancer by triggering the differentiation of immature monocytes into immunosuppressive M2-polarized macrophages [25]. Similarly, exosomal miRNA-203 derived from PC cells has been shown to promote M1 macrophage polarization while inhibiting PC cell proliferation, migration, and invasion, thereby suppressing PC progression [10].

This study elucidates the inhibitory effects of M1 macrophage-derived exosomes on the proliferation, invasion, and metastasis of PC cells *in vitro*. Moreover, exosomes derived from M1 macrophages significantly reduced PC cell growth *in vivo*. Importantly, this inhibition of PC progression is attributed to M1-exos-induced macrophage reprogramming. These findings were consistent with previous studies indicating that exosomes derived

from M1 macrophages promote M1 polarization and reprogram TAMs into M1-like macrophages by targeting IL4R, ultimately inhibiting tumor growth [15].

In summary, exosomes derived from M1 macrophages can promote TAMs to polarize into M1-like macrophages, effectively inhibiting the growth, invasion, and metastasis of PC cells, thereby exerting a suppressive role in the progression of PC. Our study not only enhances our understanding of the regulatory function of macrophages in their polarization but also elucidates the complex interactions within the innate immune microenvironment. However, the specific mechanisms need further investigation. In the future, we aim to investigate whether additional mechanisms involving macrophage exosomes in the treatment of cancer are linked to relevant signaling pathways and gene regulation.

Conclusion

M1-exos induced the polarization of TAM towards the M1 phenotype with anti-tumor potential, effectively suppressing prostate cancer growth and metastasis. Therefore, M1-exos have the potential for treating prostate cancer.

Availability of Data and Materials

The datas used and/or analyzed during the current study are available from the corresponding author.

Author Contributions

XC and LZ contributed equally to the conception and design of the research study, performed experiments, analyzed and interpreted the data, and drafted the manuscript. SC performed experiments, analyzed and interpreted the data, and critically revised the manuscript for important intellectual content. WS provided technical support in the acquisition of data, performed statistical analysis, contributed to the interpretation of the data and drafted the manuscript. HT provided expertise in the field of study, contributed to the interpretation of the data, and critically revised the manuscript for important intellectual content. XT provided guidance on the design of the research study, contributed to the interpretation of the data, and critically revised the manuscript for important intellectual content. All authors have read and approved the final manuscript, and have participated sufficiently in the work to take public responsibility for appropriate portions of the content.

Ethics Approval and Consent to Participate

This study was approved by the ethics committee of The Affiliated Nanhua Hospital, Hengyang Medical School, University of South China (No. 20230899).

Acknowledgment

Not applicable.

Funding

This study is supported by Scientific Research project of Hunan Provincial Health Commission (B202304056903).

Conflict of Interest

The authors declare no conflict of interest.

References

[1] Jemal A, Bray F, Center MM, Ferlay J, Ward E, Forman D. Global cancer statistics. CA: a Cancer Journal for Clinicians. 2011; 61: 69–90.

[2] Ju W, Zheng R, Zhang S, Zeng H, Sun K, Wang S, *et al*. Cancer statistics in Chinese older people, 2022: current burden, time trends, and comparisons with the US, Japan, and the Republic of Korea. Science China. Life Sciences. 2023; 66: 1079–1091.

[3] Pinheiro LC, Soroka O, Kern LM, Higgason N, Leonard JP, Safford MM. Racial disparities in diabetes care among incident breast, prostate, and colorectal cancer survivors: a SEER Medicare study. Journal of Cancer Survivorship: Research and Practice. 2022; 16: 52–60.

[4] Sur S, Steele R, Shi X, Ray RB. miRNA-29b Inhibits Prostate Tumor Growth and Induces Apoptosis by Increasing Bim Expression. Cells. 2019; 8: 1455.

[5] Boutilier AJ, Elsawa SF. Macrophage Polarization States in the Tumor Microenvironment. International Journal of Molecular Sciences. 2021; 22: 6995.

[6] Chen D, Zhang X, Li Z, Zhu B. Metabolic regulatory crosstalk between tumor microenvironment and tumor-associated macrophages. Theranostics. 2021; 11: 1016–1030.

[7] Kim SH, Saeidi S, Zhong X, Gwak SY, Muna IA, Park SA, *et al*. Breast cancer cell debris diminishes therapeutic efficacy through heme oxygenase-1-mediated inactivation of M1-like tumor-associated macrophages. Neoplasia (New York, N.Y.). 2020; 22: 606–616.

[8] Mantovani A, Marchesi F, Malesci A, Laghi L, Allavena P. Tumour-associated macrophages as treatment targets in oncology. Nature Reviews. Clinical Oncology. 2017; 14: 399–416.

[9] Biswas SK, Mantovani A. Macrophage plasticity and interaction with lymphocyte subsets: cancer as a paradigm. Nature Immunology. 2010; 11: 889–896.

[10] Zhang LS, Chen QC, Zong HT, Xia Q. Exosome miRNA-203 promotes M1 macrophage polarization and inhibits prostate cancer tumor progression. Molecular and Cellular Biochemistry. 2023. (online ahead of print)

[11] Rong J, Xu L, Hu Y, Liu F, Yu Y, Guo H, *et al*. Inhibition of let-7b-5p contributes to an anti-tumorigenic macrophage phenotype through the SOCS1/STAT pathway in prostate cancer. Cancer Cell International. 2020; 20: 470.

[12] Krylova SV, Feng D. The Machinery of Exosomes: Biogenesis, Release, and Uptake. International Journal of Molecular Sciences. 2023; 24: 1337.

[13] Kuse N, Kamio K, Azuma A, Matsuda K, Inomata M, Usuki J, *et al*. Exosome-Derived microRNA-22 Ameliorates Pulmonary Fibrosis by Regulating Fibroblast-to-Myofibroblast Differentiation in Vitro and in Vivo. Journal of Nippon Medical School = Nippon Ika Daigaku Zasshi. 2020; 87: 118–128.

Journal of
BIOLOGICAL REGULATORS
and Homeostatic Agents

[14] Wang X, Zhang H, Yang H, Bai M, Ning T, Deng T, *et al*. Exosome-delivered circRNA promotes glycolysis to induce chemoresistance through the miR-122-PKM2 axis in colorectal cancer. Molecular Oncology. 2020; 14: 539–555.

[15] Gunassekaran GR, Poongkavithai Vadevoo SM, Baek MC, Lee B. M1 macrophage exosomes engineered to foster M1 polarization and target the IL-4 receptor inhibit tumor growth by reprogramming tumor-associated macrophages into M1-like macrophages. Biomaterials. 2021; 278: 121137.

[16] Zhao Y, Zheng Y, Zhu Y, Li H, Zhu H, Liu T. Docetaxel-loaded M1 macrophage-derived exosomes for a safe and efficient chemoimmunotherapy of breast cancer. Journal of Nanobiotechnology. 2022; 20: 359.

[17] Combes F, Meyer E, Sanders NN. Immune cells as tumor drug delivery vehicles. Journal of Controlled Release: Official Journal of the Controlled Release Society. 2020; 327: 70–87.

[18] Cheng L, Wang Y, Huang L. Exosomes from M1-Polarized Macrophages Potentiate the Cancer Vaccine by Creating a Pro-inflammatory Microenvironment in the Lymph Node. Molecular Therapy: the Journal of the American Society of Gene Therapy. 2017; 25: 1665–1675.

[19] Tian HY, Liang Q, Shi Z, Zhao H. Exosomal CXCL14 Contributes to M2 Macrophage Polarization through NF-κB Signaling in Prostate Cancer. Oxidative Medicine and Cellular Longevity. 2022; 2022: 7616696.

[20] Xie T, Fu DJ, Li ZM, Lv DJ, Song XL, Yu YZ, *et al*. CircSMARCC1 facilitates tumor progression by disrupting the crosstalk between prostate cancer cells and tumor-associated macrophages via miR-1322/CCL20/CCR6 signaling. Molecular Cancer. 2022; 21: 173.

[21] Faas M, Ipseiz N, Ackermann J, Culemann S, Grüneboom A, Schröder F, *et al*. IL-33-induced metabolic reprogramming controls the differentiation of alternatively activated macrophages and the resolution of inflammation. Immunity. 2021; 54: 2531–2546.e5.

[22] Morel KL, Sheahan AV, Burkhart DL, Baca SC, Boufaied N, Liu Y, *et al*. EZH2 inhibition activates a dsRNA-STING-interferon stress axis that potentiates response to PD-1 checkpoint blockade in prostate cancer. Nature Cancer. 2021; 2: 444–456.

[23] Cui J, Shan K, Yang Q, Qi Y, Qu H, Li J, *et al*. Prostaglandin E_3 attenuates macrophage-associated inflammation and prostate tumour growth by modulating polarization. Journal of Cellular and Molecular Medicine. 2021; 25: 5586–5601.

[24] Yu W, Hurley J, Roberts D, Chakrabortty SK, Enderle D, Noerholm M, *et al*. Exosome-based liquid biopsies in cancer: opportunities and challenges. Annals of Oncology: Official Journal of the European Society for Medical Oncology. 2021; 32: 466–477.

[25] Biswas S, Mandal G, Roy Chowdhury S, Purohit S, Payne KK, Anadon C, *et al*. Exosomes Produced by Mesenchymal Stem Cells Drive Differentiation of Myeloid Cells into Immunosuppressive M2-Polarized Macrophages in Breast Cancer. Journal of Immunology (Baltimore, Md.: 1950). 2019; 203: 3447–3460.